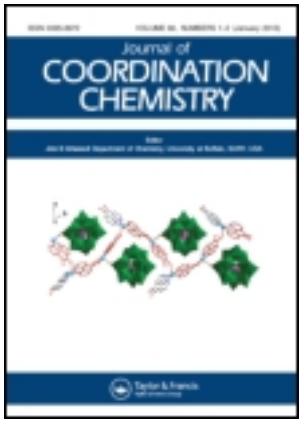

Journal of Coordination Chemistry
Publication details, including instructions for authors and subscription information:
http://www.tandfonline.com/loi/gcoo20

Synthesis, crystal structure, and DNA interaction of magnesium(II) complexes with Schiff bases

Nan Zhang [a], Yu-Hua Fan [a], Cai-Feng Bi [a], Jian Zuo [a], Peng-Fei Zhang [a], Zhong-Yu Zhang [a] & Zheng Zhu [a]

[a] Key Laboratory of Marine Chemistry Theory and Technology, Ministry of Education, College of Chemistry and Chemical Engineering, Ocean University of China, Qingdao, China

Accepted author version posted online: 15 Apr 2013.Published online: 13 May 2013.

To cite this article: Nan Zhang, Yu-Hua Fan, Cai-Feng Bi, Jian Zuo, Peng-Fei Zhang, Zhong-Yu Zhang & Zheng Zhu (2013) Synthesis, crystal structure, and DNA interaction of magnesium(II) complexes with Schiff bases, Journal of Coordination Chemistry, 66:11, 1933-1944, DOI: 10.1080/00958972.2013.796039

To link to this article: http://dx.doi.org/10.1080/00958972.2013.796039

Journal of Coordination Chemistry, 2013
Vol. 66, No. 11, 1933–1944, http://dx.doi.org/10.1080/00958972.2013.796039

Synthesis, crystal structure, and DNA interaction of magnesium(II) complexes with Schiff bases

NAN ZHANG, YU-HUA FAN, CAI-FENG BI*, JIAN ZUO, PENG-FEI ZHANG, ZHONG-YU ZHANG and ZHENG ZHU

Key Laboratory of Marine Chemistry Theory and Technology, Ministry of Education, College of Chemistry and Chemical Engineering, Ocean University of China, Qingdao, China

(*Received 17 December 2012; in final form 14 February 2013*)

A pair of stereoisomers of magnesium Schiff base complexes, $[Mg(C_{18}H_{16}N_3O_2)_2{\cdot}2CH_3OH]_n$ (**1**) ($C_{18}H_{16}N_3O_2$: 2-acetylpyridine-L-tryptophan) and $[Mg(C_{18}H_{16}N_3O_2)_2{\cdot}2CH_3OH]_n$ (**2**) ($C_{18}H_{16}N_3O_2$: 2-acetylpyridine-D-tryptophan), was synthesized and characterized by IR, UV, elemental analysis, ^{1}H NMR, and X-ray diffraction single crystal analysis. The analyses of the structures indicate that they all crystallize in the tetragonal crystal system, space group $P4_32_12$ and $P4_12_12$, respectively. The two magnesium complexes have similar crystal structures. Mg(II) is six-coordinate with two nitrogens from C=N, two nitrogens from pyridine, and two carboxylic oxygens in different ligands forming a distorted octahedral geometry. Through N–H···O intermolecular hydrogen bonds a 2-D layer structure was formed. The interaction between **1** and calf thymus DNA was also investigated by UV absorption spectra, fluorescence emission spectra and viscometry. The results indicate that **1** interacts with DNA very strongly ($K_b = 2.01 \times 10^7\,L\,mol^{-1}$ and $K_{sq} = 0.195$). The nature of the binding seems to be mainly an electrostatic interaction between DNA and the magnesium complex. Other binding modes, such as hydrogen bonds, may also exist.

Keywords: Tryptophan; 2-Acetylpyridine; Schiff base; Crystal structure; DNA interaction

1. Introduction

Amino acids contain an amine, a carboxylic acid, and a side chain that varies with different amino acids. They are critical to life and have many functions in metabolism. One particularly important function is to serve as building blocks of proteins [1]. Amino acids often act as the essential ingredients of coenzymes and the precursors of heme, which play key roles in biochemistry [2, 3].

Amino acids react with carbonyl compounds to form Schiff bases [4–6]. There has been considerable interest in metal complexes with Schiff bases. Schiff base complexes have a variety of applications including biology [7–9], magnetism [10, 11], medical imaging [12, 13], and catalysis [14–16]. DNA is an important genetic material, playing an important role in storage, copying and transmission of genetic messages. Serving as a target molecule, recognition of DNA for natural and artificial molecules in the inhibition of cellular

*Corresponding author. Email: bicaifeng301@163.com

disorders and in therapy of certain diseases is of paramount importance in inorganic biochemistry. Many transition metal complexes have been synthesized and the interactions between complexes and DNA are studied [17–20]. However, the structures of alkaline earth complexes and their interactions with DNA have been rarely reported. In the present study, we describe the preparations and crystal structures of two magnesium complexes with Schiff bases $[Mg(C_{18}H_{16}N_3O_2)_2{\cdot}2CH_3OH]_n$ (**1**), which was derived from 2-acetylpyridine-L-tryptophan, and $[Mg(C_{18}H_{16}N_3O_2)_2{\cdot}2CH_3OH]_n$ (**2**), which was derived from 2-acetylpyridine-D-tryptophan. Finally, the interaction of **1** with DNA was studied by UV absorption spectra, fluorescence emission spectra, and viscometry.

2. Experimental

2.1. *Materials and measurements*

Calf thymus DNA (CT-DNA) and ethidium bromide (EB) were obtained from Sigma-Aldrich Co.(USA). The other reagents used in this work were of analytical grade and all chemicals were used without purification. The 2-acetylpyridine was purchased from Acros and the L- and D-tryptophan were purchased from Aladdin. The other chemicals were produced in China. The experiments involving interaction of the magnesium complex with CT-DNA were carried out in Milli-Q water buffer containing $5\,mM\,L^{-1}$ Tris and $50\,mM\,L^{-1}$ NaCl, and adjusted to pH 7.2 with hydrochloric acid. A solution of CT-DNA gave a ratio of UV absorbance at 260 and 280 nm of about 1.8–1.9, indicating that the CT-DNA was sufficiently free of protein [21]. The CT-DNA concentration per nucleotide was determined spectrophotometrically by employing an extinction coefficient of $6600\,L\,M^{-1}\,cm^{-1}$ at 260 nm [22].

Infrared spectra were recorded as KBr pellets on the Nicolet 170SX spectrophotometer from 4000 to $400\,cm^{-1}$. UV spectra were performed on a Unicam UV2 spectrometer. Elemental analysis was carried out on a Carlo Erba 1106 full-automatic trace organic elemental analyzer and ^1H NMR spectra were obtained on a Bruker DRX-600 spectrometer. X-ray diffraction data were collected on an Enraf-Nonius CAD-4 diffractometer. Fluorescence spectra were measured with a Hitachi F-4500 spectrophotometer. Viscosity measurements were conducted using an Ubbelodhe viscometer.

2.2. *Synthesis of 1 and 2*

2.2.1. $[Mg(C_{18}H_{16}N_3O_2)_2{\cdot}2CH_3OH]_n$ (1). L-tryptophan (0.408 g, 2.0 mM) and potassium hydroxide (0.112 g, 2.0 mM) were dissolved in 50 mL of methanol with magnetic stirring, and then 2.0 mM (0.242 g) of 2-acetylpyridine was added dropwise to the solution. The reaction mixture was heated to 50 °C with stirring and then refluxed for 6 h to give a bright orange solution. After that, 10 mL of methanol solution of $MgCl_2{\cdot}6H_2O$ (0.203 g, 1.0 mM) was added to 50 mL of methanol solution of the ligand (0.691 g, 2.0 mM), and the mixture was stirred and refluxed at 50 °C for 6 h. The resulting solution was cooled at room temperature and then filtered. The filtrate was left for slow evaporation at room temperature. Yellow block-shaped crystals were formed two days later with 69% yield on L-tryptophan. Elemental Anal. Calcd (%) for $[Mg(C_{18}H_{16}N_3O_2)_2{\cdot}2CH_3OH]_n$ (**1**): C, 65.10;

H, 5.75; N, 11.99. Found: C, 64.97; H, 5.83; N, 12.14. IR (KBr, cm^{-1}): 1646 (vs), 1610 (vs), 1438 (s), 1373 (vs), 1311 (s), 1250 (s), 1160 (w), 1136 (vw), 1103 (w), 1042 (vw), 1009 (m), 976 (vw), 919 (w), 874 (w), 784 (s), 751 (vs), 698 (s), 670 (w), 641 (vw), 580 (m), 506 (w), 465 (vw), 412 (m). ^{1}H NMR (DMSO-d6 600 MHz) δ (ppm): 1.42 (s, 3H), 3.15 (t, 1H, J = 12.0 Hz), 3.53 (d, 1H, J = 13.2 Hz), 4.49 (d, 1H, J = 8.4 Hz), 6.80 (t, 1H, J = 7.2 Hz), 7.02 (t, 1H, J = 7.8 Hz), 7.06 (s, 1H), 7.34 (d, 1H, J = 7.8 Hz), 7.38 (s, 1H), 7.63 (d, 2H, J = 7.2 Hz), 7.92 (s, 1H), 8.02 (s, 1H), 10.91 (s, 1H).

2.2.2. $[Mg(C_{18}H_{16}N_3O_2)_2{\cdot}2CH_3OH]_n$ (2). Complex **2** was synthesized in a procedure similar to that of **1**, but using D-tryptophan instead of L-tryptophan. Yellow block crystals of **2** were obtained one day later (yield 64% based on D-tryptophan). The synthesis of **1** and **2** is shown in Scheme 1. Elemental Anal. Calcd (%) for $[Mg(C_{18}H_{16}N_3O_2)_2{\cdot}2CH_3OH]_n$ (**2**): C, 65.10; H, 5.75; N, 11.99. Found: C, 64.86; H, 5.94; N, 12.07. IR (KBr, cm^{-1}): 1646 (vs), 1610 (vs), 1434 (s), 1373 (vs), 1311 (s), 1250 (s), 1160 (w), 1136 (w), 1099 (w), 1042 (w), 1005 (m), 976 (vw), 919 (w), 870 (w), 784 (s), 751 (vs), 694 (s), 637 (w), 612 (w), 580 (m), 510 (w), 457 (vw), 416 (m). ^{1}H NMR (DMSO-d6 600 MHz) δ (ppm): 1.42 (s, 3H), 3.15 (t, 1H, J = 11.4 Hz), 3.54 (d, 1H, J = 13.2 Hz), 4.49 (d, 1H, J = 8.4 Hz), 6.80 (t, 1H, J = 7.2 Hz), 7.02 (t, 1H, J = 7.8 Hz), 7.06 (s, 1H), 7.34 (d, 1H, J = 8.2 Hz), 7.38 (s, 1H), 7.63 (d, 2H, J = 7.2 Hz), 7.92 (s, 1H), 8.01 (s, 1H), 10.91 (s, 1H).

2.3. *Crystallographic data collection and structure determination*

Single crystals were mounted on an Enraf-Nonius CAD-4 X-ray single-crystal diffractometer. All data were collected at 293(2) K with graphite monochromated Mo$K\alpha$ radiation (λ = 0.71073 Å) in ω-2θ scan mode. The structures were solved by direct methods using SHELXS-97 [23]. Nonhydrogen atoms were defined by the Fourier synthesis method. Positional and thermal parameters were refined by full matrix least-squares (on F^2) to convergence. A summary of the key crystallographic information is given in table 1, selected bond lengths and angles are listed in table 2, and hydrogen bonds can be found in table 3.

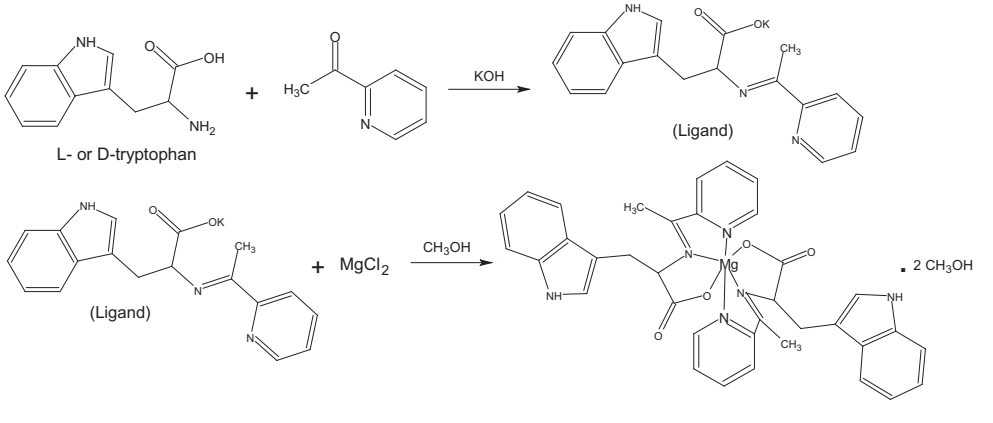

Scheme 1. The synthesis of **1** and **2**.

Table 1. Crystallographic data and X-ray experiment details for **1** and **2**.

Parameter	**1**	**2**
Identification code	$[Mg(C_{18}H_{16}N_3O_2)_2{\cdot}2CH_3OH]_n$	$[Mg(C_{18}H_{16}N_3O_2)_2{\cdot}2CH_3OH]_n$
Empirical formula	$C_{38}H_{40}N_6O_6Mg$	$C_{38}H_{40}N_6O_6Mg$
Formula weight	701.07	701.07
Crystal system	Tetragonal	Tetragonal
Space group	$P4_32_12$	$P4_12_12$
a/Å	11.6532(14)	11.8234(11)
b/Å	11.6532(14)	11.8234(11)
c/Å	29.025(3)	28.817(3)
α/deg	90	90
β/deg	90	90
γ/deg	90	90
Volume/Å^3	3941.5(8)	4028.5(6)
$F(0\,0\,0)$	1480	1480
Crystal size/mm	$0.40 \times 0.37 \times 0.32$	$0.45 \times 0.40 \times 0.37$
θ range for data collection/deg	2.24–25.01	2.54–25.02
Limiting indices	$-12 \leqslant h \leqslant 13$ $-13 \leqslant k \leqslant 13$ $-34 \leqslant l \leqslant 27$	$-14 \leqslant h \leqslant 11$ $-13 \leqslant k \leqslant 14$ $-34 \leqslant l \leqslant 34$
Reflections collected/unique	19,606/3476 ($R_{int} = 0.0978$)	20,583/3530 ($R_{int} = 0.0517$)
ρ_{calcd}/g cm^{-3}	1.181	1.156
Data/restraints/parameters	3476/0/252	3530/0/253
Goodness of fit on F^2	1.054	1.080
Final R indices ($I > 2\sigma(I)$)	$R_1 = 0.0670$, $wR_2 = 0.1763$	$R_1 = 0.0565$, $wR_2 = 0.1481$
R indices (all data)	$R_1 = 0.1443$, $wR_2 = 0.2076$	$R_1 = 0.1104$, $wR_2 = 0.1992$
Largest diff. peak and hole/e Å^{-3}	0.285 and −0.158	0.284 and −0.231

Notes: (**1**) $w = 1/[\sigma^2 (F_0^2) + (0.0918)^2]$, with $P = (F_0^2 + 2F_c^2)/3$. (**2**) $w = 1/[\sigma^2 ((F_0^2) + (0.1091P)^2 + 0.4903P]$, with $P = (F_0^2 + 2F_c^2)/3$.

The molecular structures and crystal packing diagrams of the two magnesium complexes are shown in figure 1 and figures S1–S3 (in Supplementary material).

2.4. *DNA-binding studies*

2.4.1. Ultraviolet spectral measurements. Complex **1** was dissolved in a mixture of DMSO and Tris–HCl buffer. Absorption titration experiments were carried out by gradually increasing the DNA concentration and maintaining the complex concentration at 5×10^{-8} M L^{-1}. Absorbances were recorded after each successive addition of DNA solution and equilibration.

2.4.2. Fluorescence spectral measurements. Fluorescence spectral measurements was carried out by successive additions of **1** (0.5–3.5 $\times 10^{-6}$ M L^{-1}) to DNA (2.5×10^{-6} M L^{-1}) containing EB (2.5×10^{-6} M L^{-1}) in Tris–HCl buffer. The scanner speed was 1200 nm min^{-1} and the slit width was 5 nm. These samples were excited at 268 nm.

2.4.3. Viscosity measurements. Viscosity measurements were conducted using an Ubbelodhe viscometer, which was immersed in a thermostated water bath maintained to 298 (±0.1) K. Titrations were performed for the complex which can be introduced into a

Table 2. Bond lengths (Å) and angles (°) for **1** and **2**.

$[Mg(C_{18}H_{16}N_3O_2)_2{\cdot}2CH_3OH]_n$ (**1**)			
Mg(1)–O(1)	2.026(4)	Mg(1)–N(3)	2.180(5)
Mg(1)–O(1) #1	2.026(4)	Mg(1)–N(3) #1	2.180(5)
Mg(1)–N(1)	2.145(4)	N(1)–C(13)	1.293(6)
Mg(1)–N(1A)	2.145(4)		
O(1A)–Mg(1)–O(1)	94.2(2)	N(1)–Mg(1)–N(3A)	73.93(17)
O(1A)–Mg(1)–N(1)	99.28(17)	N(1A)–Mg(1)–N(3A)	111.03(17)
O(1)–Mg(1)–N(1)	76.04(18)	O(1A)–Mg(1)–N(3)	149.62(17)
O(1A)–Mg(1)–N(1A)	76.04(18)	O(1)–Mg(1)–N(3)	94.97(15)
O(1)–Mg(1)–N(1A)	99.28(17)	N(1)–Mg(1)–N(3)	111.03(18)
N(1)–Mg(1)–N(1A)	173.3(3)	N(1A)–Mg(1)–N(3)	73.93(17)
O(1A)–Mg(1)–N(3A)	94.97(15)	N(3A)–Mg(1)–N(3)	91.5(2)
O(1)–Mg(1)–N(3A)	149.62(17)		
$[Mg(C_{18}H_{16}N_3O_2)_2{\cdot}2CH_3OH]_n$ (**2**)			
Mg(1)–O(1)	2.034(3)	Mg(1)–N(3)	2.209(4)
Mg(1)–O(1A)	2.034(3)	Mg(1)–N(3A)	2.209(4)
Mg(1)–N(1)	2.156(3)	N(1)–C(13)	1.277(5)
Mg(1)–N(1A)	2.156(3)		
O(1)–Mg(1)–O(1A)	94.04(19)	N(1)–Mg(1)–N(3A)	73.74(13)
O(1)–Mg(1)–N(1)	76.56(13)	N(1A)–Mg(1)–N(3A)	111.49(13)
O(1A)–Mg(1)–N(1)	98.50(13)	O(1)–Mg(1)–N(3)	94.81(13)
O(1)–Mg(1)–N(1A)	98.50(13)	O(1A)–Mg(1)–N(3)	149.94(12)
O(1A)–Mg(1)–N(1A)	76.56(13)	N(1)–Mg(1)–N(3)	111.49(13)
N(1)–Mg(1)–N(1A)	172.9(2)	N(1A)–Mg(1)–N(3)	73.74(13)
O(1)–Mg(1)–N(3A)	149.94(12)	N(3A)–Mg(1)–N(3)	91.7(2)
O(1A)–Mg(1)–N(3A)	94.81(13)		

Symmetry transformations used to generate equivalent atoms: A: $y, x, -z$.

Table 3. Hydrogen bonds for **1** and **2** (Å or °).

D–H···A	d(D–H)	d(H···A)	d(D···A)	∠DHA
$[Mg(C_{18}H_{16}N_3O_2)_2{\cdot}2CH_3OH]_n$ (**1**)				
N(2)–H(2)···O(1)	0.860	2.074	2.822	144.97
O(3)–H(3)···O(2)	0.820	2.069	2.834	154.99
O(3)–H(3)···O(4)	0.820	2.558	3.167	132.20
O(4)–H(4)···O(2)	0.820	1.945	2.754	168.89
Symmetry transformations used to generate equivalent atoms: $x+1/2, -y+3/2, -z+¼$				
$[Mg(C_{18}H_{16}N_3O_2)_2{\cdot}2CH_3OH]_n$ (**2**)				
N(2)–H(2)···O(1)	0.860	2.059	2.809	145.28
O(3)–H(3a)···O(2)	0.820	1.892	2.711	176.79
O(3′)–H(3′b)···O(2)	0.820	1.944	2.751	167.68
Symmetry transformations used to generate equivalent atoms: $-x+1/2, y-1/2, -z+¼$				

DNA solution in the viscometer. Data were presented as $(\eta/\eta_0)^{1/3}$ *versus* the ratio of the concentration of the complex and DNA, where η is the viscosity of DNA in the presence of the complex and η_0 is the viscosity of DNA alone.

3. Results and discussion

3.1. *Structural descriptions of 1 and 2*

Since the two magnesium complexes were a pair of stereoisomers and derived from two similar ligands of 2-acetylpyridine-L-tryptophan and 2-acetylpyridine-D-tryptophan, they

have similar structures. Crystallographic structural analysis reveals that both magnesium crystals crystallize in the tetragonal crystal system, space groups $P4_32_12$ and $P4_12_12$, respectively. Each magnesium coordinates with two Schiff base ligands, two nitrogens from C=N, two nitrogens from pyridine, and two carboxylic oxygens in different ligands, forming a 4N + 2O neutral complex. There are two solvent methanols in the crystalline lattice which are not bound to metal.

The crystal structure of **1** is shown in figure 1. The corresponding bond angles of O(1A) Mg(1)N(3) (149.62°) and O(1)Mg(1)N(3A) (149.62°) (table 2) are less than 180°, and the bond angles N(1A)Mg(1)O(1) (99.28°), N(1A)Mg(1)N(3) (73.93°), N(1A)Mg(1)O(1A) (76.04°), and N(1A)Mg(1)N(3A) (111.03°) indicate that Mg(II) adopts a distorted octahedral geometry. N(3), O(1), O(1A), and N(3A) occupy each vertex of the basal site, while N(1) and N(1A) locate in apical positions of the octahedral structure. The bond length of C(13)–N(1) is 1.293 Å, which is close to normal C=N 1.306 Å [24], indicating a double bond between C(13) and N(1) in the complex. The bond lengths of Mg(1)–O(1) and Mg (1)–O(1A) are both 2.026 Å, in agreement with the relative values of Mg–O in the literature [25]. Mg–N, Mg(1)–N(1) (2.145 Å), Mg(1)–N(1A) (2.145 Å), are shorter than Mg(1)–N(3) (2.180 Å) and Mg(1)–N(3A) (2.180 Å), suggesting that coordination ability of N(1) and N (1A) in imines is stronger than that of N(3) and N(3A) in pyridine rings. Each ligand serves as a bridge linking Mg(II) ions through N–H···O intermolecular hydrogen bonds, leading to a 1-D coordination polymer (figure 2). Two adjacent chains are bridged by N–H···O hydrogen bonds. The N(2)–O(1) distance is 2.822 Å and the angle is 144.97° (symmetry code: $x+1/2, -y+3/2, -z+1/4$). As a result of the alternate arrangement of chains through inter-chained hydrogen bonding interactions, a 2-D layer is formed (figure 3).

Bond lengths of Mg(1)–O(1) (2.034 Å), Mg(1)–N(1) (2.156 Å), and Mg(1)–N(3) (2.209 Å) in $[Mg(C_{18}H_{16}N_3O_2)_2{\cdot}2CH_3OH]_n$ (**2**) are a little longer than those of $[Mg(C_{18}H_{16}N_3O_2)_2{\cdot}2CH_3OH]_n$ (**1**), showing that the coordination ability of Mg–O and Mg–N in **1** is weaker than that of **2**.

Magnesium complexes with NNO Schiff-base ligands consistently yield distorted octahedral coordination geometry [26]. In those structures, the Mg–O bonds (2.0055–2.246 Å) were shorter than the ones reported here, and Mg–N bonds (2.1169–2.3284 Å, both the imine and quinoline donor) were shorter or longer than those of our magnesium

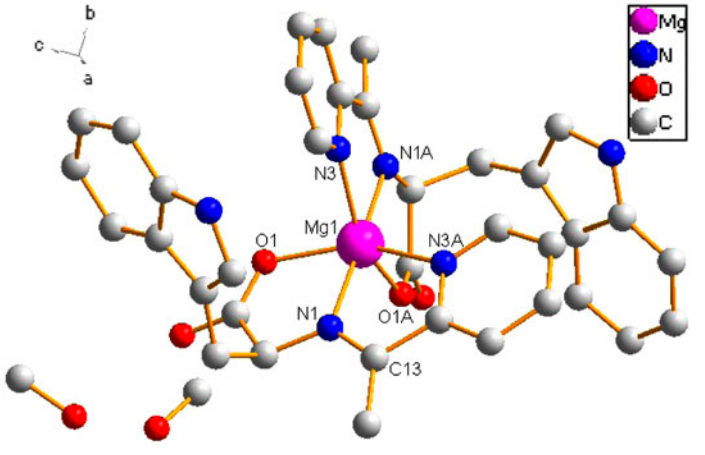

Figure 1. Crystal structure of $[Mg(C_{18}H_{16}N_3O_2)_2{\cdot}2CH_3OH]_n$ (**1**). All hydrogens were omitted for clarity.

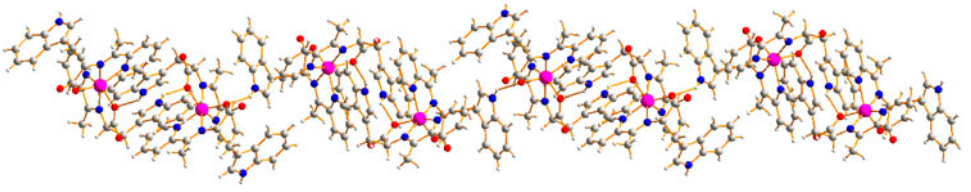

Figure 2. 1-D chain structure of **1** linked by N–H···O hydrogen bonds.

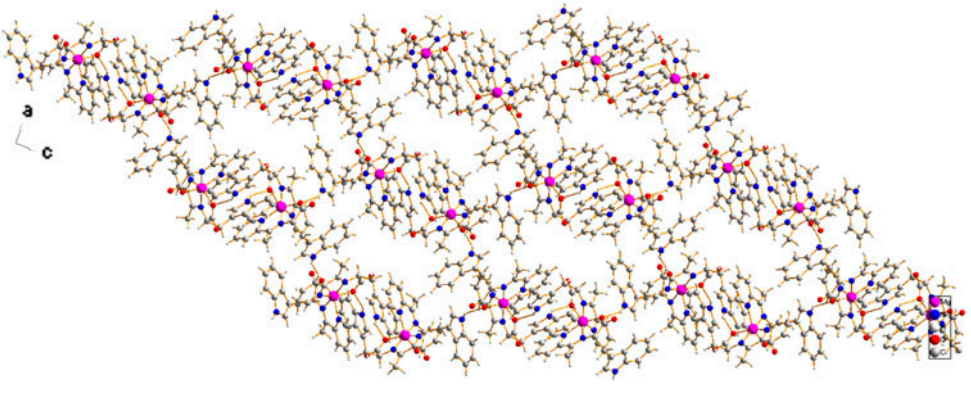

Figure 3. 2-D layer structure of **1**.

complexes, likely resulting from flexibility derived from the two bridging ligands. Similarly, small bite angles for the O–Mg–N(imine) 84–87° and N(quinoline)–Mg–N(imine) 73–76° were reported. These bond angles compare favorably to those reported here.

3.2. *Spectroscopy description of 1 and 2*

Figure S4 in supplementary material shows the UV spectra of the ligands and their complexes in methanol. There are two absorptions at 221, 221 and 273, and 272 nm from 210 to 300 nm in the spectra of the ligands of 2-acetylpyridine-L-tryptophan (L1) and 2-acetylpyridine-D-tryptophan (L2), respectively. The counterparts of **1** and **2** appear at 221, 221 and 280, and 279 nm, respectively. The first peaks are assigned to the π–π^* transition of the pyridyl or indol. The second peaks are assigned to the n–π^* transition and the conjugation between a lone pair electron of the N in the C=N group and delocalized π bond of the aromatic ring. The shifts of 7 nm are caused by coordination of N to magnesium, providing evidence for coordination [27].

3.3. *DNA-binding studies*

3.3.1. Ultraviolet spectral measurements. Electronic absorption spectra are employed to study the binding of **1** with CT-DNA. In the UV region, the absorption bands at 206 nm for **1** can be attributed to π–π^* transition of the coordinated ligands. Addition of increasing amounts of CT-DNA results in hyperchromism and slight blue shift of the

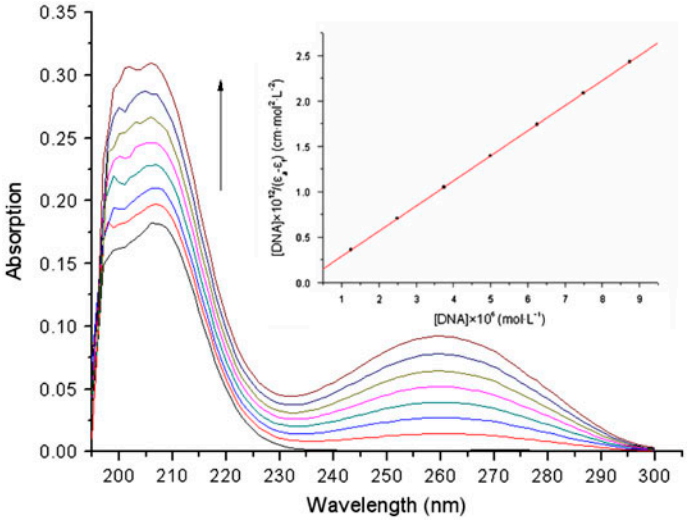

Figure 4. Absorption spectra of **1** in the absence and presence of increasing amounts of DNA. [Complex] $= 5 \times 10^{-8}$ M L^{-1}, [DNA] = 1.25–8.75 $\times 10^{-6}$ M L^{-1}. Arrow shows the absorbance change upon increasing DNA concentration. Inset: plot of [DNA]/($\varepsilon_a - \varepsilon_f$) *vs.* [DNA].

absorption bands (figure 4). An electrostatic interaction between CT-DNA and **1** can be predicted based on the hyperchromism exhibited and shift in absorbance. Since each complex has two pyridine and two indoline rings, located at different planes, the magnesium complex is nonplanar and classical intercalation is precluded [28]. As the DNA double helix possesses many hydrogen bonding sites which are accessible both in the minor and major grooves, it is likely that N–H in indoline ring of the complex forms hydrogen bonds with N of adenine or O of thymine in the DNA [29]. Because, so many pyridine and indoline rings exist in the magnesium complex, it could form hydrogen bonds between aromatic rings of the complex and DNA, contributing to the hyperchromism observed in absorption spectra [30, 31].

The intrinsic binding constant of **1** with DNA was determined by the equation $[\mathrm{DNA}]/(\varepsilon_a - \varepsilon_f) = [\mathrm{DNA}]/(\varepsilon_b - \varepsilon_f) + 1/K_b(\varepsilon_b - \varepsilon_f)$ [32], where [DNA] is the concentration of DNA in base pairs, K_b is the intrinsic binding constant, ε_a corresponds to the apparent extinction coefficient, and ε_b and ε_f correspond to the extinction coefficient of the bound form of complex and the extinction coefficient of free complex, respectively. A summary of the data from the equation for the interaction between **1** and DNA is given in table 4. The ratio of slope to intercept in the plot of [DNA]/($\varepsilon_a - \varepsilon_f$) *versus* [DNA] gives

Table 4. Data from the equation for the interaction between **1** and DNA.

[DNA]/(10^{-6} M L^{-1})	Wavelength/nm	Absorption	ε_a/(10^4 L M^{-1} cm^{-1})	[DNA]/(|ε_a-ε_f|)/(10^{-12} cm M^2 L^{-2})
0	206	0.18188	–	–
1.25	207	0.19744	15.7952	0.3592
2.5	207	0.21035	8.4140	0.7035
3.75	207	0.22857	6.0952	1.0485
5	207	0.24607	4.9214	1.3934
6.25	206	0.26683	4.2693	1.7386
7.5	206	0.28727	3.8303	2.0837
8.75	207	0.30923	3.5340	2.4290

the value of K_b as $2.01 \times 10^7\,L\,M^{-1}$. This K_b value for **1** is much higher than that for other complexes like Mg(II)L(H_2O)·$2H_2O$ (K_b, $2.9 \times 10^5\,L\,M^{-1}$) [33], showing that our magnesium complex binds very strongly with CT-DNA.

3.3.2. Fluorescence spectral measurements. EB is a well-known cationic dye commonly used as a fluorescent probe for native DNA [34]. The fluorescence intensity of EB is very weak, but greatly increases when EB is intercalated into the base pairs of double-stranded DNA. Intercalative binding between a complex and DNA could cause replacement of EB, leading to a fluorescence quenching. Classical electrostatic interaction may make contract DNA by neutralizing negative charges of phosphate groups in DNA, squeezing EB out of DNA and also resulting in fluorescence quenching [35, 36]. Figure 5 shows that with the increase of concentration of magnesium complex, there is an obvious hypochromic effect on the fluorescence spectra and quenching of fluorescence intensity of the DNA-EB system. We calculated the quenching constant K_{sq} according to the classical Stern–Volmer equation [37], $I_0/I = 1 + K_{sq} \cdot r$, where I_0 is the emission intensity in the absence of quencher, I is the emission intensity in the present of quencher, and r corresponds to [Complex]/[DNA]. The data from the Stern–Volmer equation for the interaction between **1** and DNA-EB system are given in table 5. The quenching plot illustrates that the quenching of EB bound to DNA by **1** is in agreement with the linear Stern–Volmer equation, which also indicates that the complex binds to DNA. The K_{sq} value (0.195) given by the ratio of the slope to intercept is higher than that for other magnesium complexes [38], suggesting that our magnesium complex binds strongly with DNA, consistent with our electronic absorption spectral results.

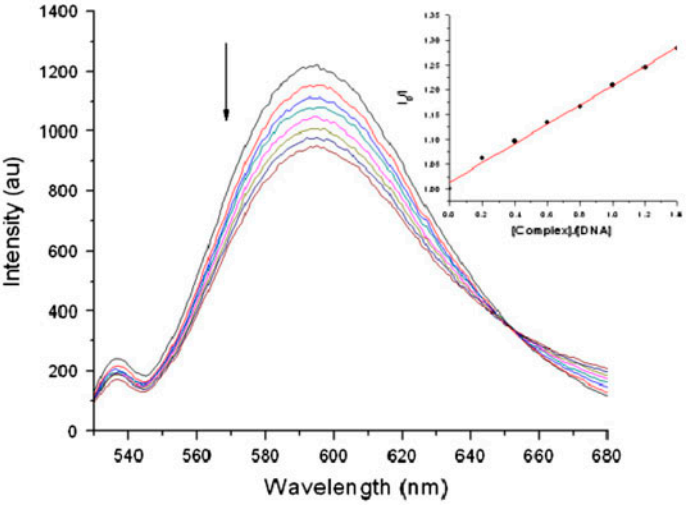

Figure 5. Relative fluorescence intensity of EB bound to DNA in the absence and presence of **1**. [EB] $= 2.5 \times 10^{-6}\,M\,L^{-1}$, [DNA] $= 2.5 \times 10^{-6}\,M\,L^{-1}$, [Complex] $= 0$–$3.5 \times 10^{-6}\,M\,L^{-1}$. Inset: plot of I_0/I *vs.* [Complex]/[DNA].

Table 5. Data from the Stern–Volmer equation for interaction between **1** and DNA–EB system.

[Complex]/(10^{-6} M L^{-1})	Wavelength/nm	Intensity/au	r	I_0/I
0	595.0	1224	–	–
0.5	592.8	1153	0.2	1.062
1.0	594.6	1116	0.4	1.097
1.5	592.8	1080	0.6	1.133
2.0	594.8	1049	0.8	1.167
2.5	594.8	1012	1.0	1.209
3.0	592.8	982	1.2	1.246
3.5	594.6	954	1.4	1.283

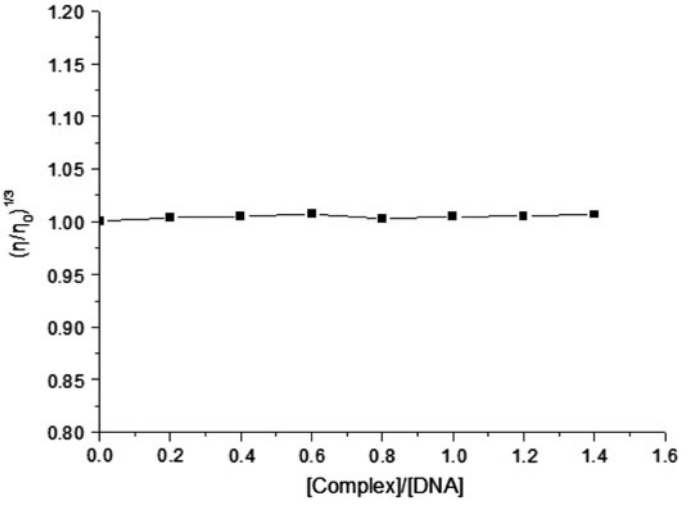

Figure 6. Effects of increasing amounts of **1** on the relative viscosities of DNA. [DNA] = 5×10^{-6} M L^{-1}, [Complex] = 1–7×10^{-6} M L^{-1}.

3.3.3. Viscosity measurements. Viscosity, sensitive to volume increases, is regarded as one of the least ambiguous and most critical tests of binding interactions with DNA in solution in the absence of crystallographic structural data [39]. To further confirm the interaction mode between **1** and DNA, a viscosity study was carried out. Classical intercalation is known to cause a significant increase in the viscosity of a DNA solution, as base pairs are separated to accommodate the binding ligand. In contrast, a partial intercalation mode could bend (or kink) the DNA helix, resulting in decrease of the effective length and viscosity. Other binding causes no obvious increase of DNA viscosity [21, 40].

As shown in figure 6, the specific viscosity of DNA can be considered to remain invariable with increased concentration of **1**, which supports the studies suggesting that the complexes interact with DNA via electrostatic interaction mode.

4. Conclusion

We synthesized and characterized two magnesium complexes, $[Mg(C_{18}H_{16}N_3O_2)_2 \cdot 2CH_3OH]_n$ (**1**) ($C_{18}H_{16}N_3O_2$: 2-acetylpyridine-L-tryptophan) and $[Mg(C_{18}H_{16}N_3O_2)_2 \cdot 2$-

$CH_3OH]_n$ (**2**) ($C_{18}H_{16}N_3O_2$: 2-acetylpyridine-D-tryptophan), which are a pair of stereoisomers. They crystallize in the tetragonal crystal system, space groups $P4_32_12$ and $P4_12_12$, respectively. Both are six-coordinate by two nitrogens from C=N, two nitrogens from pyridine and two carboxylic oxygens in different ligands, forming a distorted octahedron. The complexes display a 2-D coordination polymer through N–H···O intermolecular hydrogen bonds. The interaction between **1** and CT-DNA was also investigated by UV absorption spectra, fluorescence emission spectra and viscometry. The results indicate that **1** binds to DNA in an electrostatic mode; hydrogen bonds may also exist in this system.

Supplementary material

Crystallographic information of the Schiff base coordination complexes have been deposited with the Cambridge Crystallographic Data Center as supplementary publication numbers (CCDC 828384 and 830565). Copies of the data may be obtained free of charge on application to CCDC, 12 Union Road, Cambridge CB2 1 EB, UK (Fax: +44-1223-336–033; E-mail: deposit@ccdc.cam.ac.uk or http://www.ccdc.cam.ac.uk).

Acknowledgements

We would like to thank Madhu Sanam (Wayne State University, USA) for the critical reading of this manuscript. This work was supported by the National Science Foundation of China (Nos. 21071134 and 20971115).

References

[1] S. Mho, D.C. Johnson. *J. Electroanal. Chem.*, **495**, 152 (2001).
[2] T. Hokfelt. *Neuron*, **7**, 867 (1991).
[3] K.L. Kostel, S.M. Lunte. *J. Chromatogr. B*, **27**, 695 (1997).
[4] K. Dey, A.K. Biswas, A. Roy. *Indian J. Chem., Sect A*, **20**, 848 (1981).
[5] R.V. Rao, C.P. Rao, E.K. Wegelius. *J. Chem. Crystallogr.*, **33**, 139 (2003).
[6] Y.H. Fan, Y.N. Zou, C.F. Bi, A.D. Wang, F. Guo. *Russ. J. Coord. Chem.*, **33**, 570 (2007).
[7] N. Zhang, Y.H. Fan, Z. Zhang, J. Zuo, P.F. Zhang, Q. Wang, S.B. Liu, C.F. Bi. *Inorg. Chem. Commun.*, **22**, 68 (2012).
[8] X. Zhang, M. Frezza, V. Milacic, L. Ronconi, C.F. Bi, D. Fregona, Q.P. Dou. *J. Cell. Biochem.*, **109**, 162 (2010).
[9] Y. Xiao, C.F. Bi, Y.H. Fan, S.B. Liu, X. Zhang, D.M. Zhang, Y.L. Wang, R. Zhu. *J. Coord. Chem.*, **62**, 3029 (2009).
[10] F.M. Nie, Z.Y. Dong, F. Lu, G.X. Li. *J. Coord. Chem.*, **63**, 4259 (2010).
[11] A.A. Nejo, G.A. Kolawole, M.C. Dumbele, A.R. Opoku. *J. Coord. Chem.*, **63**, 4367 (2010).
[12] P. Mukherjee, C. Biswas, M.G.B. Drew, A. Ghosh. *Polyhedron*, **26**, 3121 (2007).
[13] X. Zhang, C.F. Bi, Y.H. Fan, Q.Z. Cui, D. Chen, Y. Xiao, Q.P. Dou. *Int. J. Mol. Med.*, **22**, 677 (2008).
[14] E. Kimura, S. Wada, M. Shiyonoya, Y. Okazaki. *Inorg. Chem.*, **96**, 770 (1994).
[15] F. Heshmatpour, S. Rayati, M.A. Hajiabbas, B. Neumüller. *Z. Anorg. Allg. Chem.*, **637**, 1224 (2011).
[16] K.C. Gupta, A.K. Star. *Coord. Chem. Rev.*, **252**, 1420 (2008).
[17] P.S. Guin, P.C. Mandal, S. Das. *J. Coord. Chem.*, **65**, 705 (2012).
[18] G. Raja, R.J. Butcher, C. Jayabalakrishnan. *Transition Met. Chem.*, **37**, 169 (2012).
[19] F.L. Thorp-Greenwood, M.P. Coogan, L. Mishra, N. Kumari, G. Rai, S. Saripella. *New J. Chem.*, **36**, 64 (2012).
[20] N. Raman, A. Sakthivel, R. Jeyamurugan. *J. Coord. Chem.*, **63**, 4380 (2010).
[21] S. Satyanarayana, J.C. Dabrowiak, J.B. Chaires. *Biochemistry*, **32**, 2573 (1993).
[22] M.F. Reichmann, S.A. Rice, C.A. Thomas, P. Doty. *J. Am. Chem. Soc.*, **76**, 3047 (1954).

[23] G.M. Sheldrick. *SHELXL-97, Program for Crystal Structure Analysis*, University of Göttingen, Germany (1997).
[24] Y.H. Fan, Y.F. Wang, C.F. Bi, Q. Wang, X. Zhang, X.Y. Liu. *Russ. J. Coord. Chem.*, **36**, 509 (2010).
[25] G.T. Quinque, A.G. Oliver, J.A. Rood. *Eur. J. Inorg. Chem.*, **22**, 3321 (2011).
[26] C.C. Roberts, J.M. Fritsch. *Polyhedron*, **29**, 1271 (2010).
[27] N. Zhang, Y.H. Fan, C.F. Bi, J. Zuo, Q. Wang. *Russ. J. Coord. Chem.*, **38**, 349 (2012).
[28] M.T. Carter, M. Rodriguez, A.J. Bard. *J. Am. Chem. Soc.*, **111**, 8901 (1989).
[29] B.E. Chen, H.C. Liu, X.X. Sun, C.G. Yang. *Mol. BioSyst.*, **6**, 2143 (2010).
[30] R.S. Kumar, S. Arunachalam. *Polyhedron*, **25**, 3113 (2006).
[31] R.S. Kumar, S. Arunachalam. *Eur. J. Med. Chem.*, **44**, 1878 (2009).
[32] A. Wolfe, G.H. Shimer, T. Meehan. *Biochemistry*, **26**, 6392 (1987).
[33] Y. Zhang, X. Wang, L. Ding. *Nucleos. Nucleot. Nucl.*, **30**, 49 (2011).
[34] J. Olmsted, D.R. Kearns. *Biochemistry*, **16**, 3647 (1977).
[35] J.B. Lepecq, C. Paoletti. *J. Mol. Biol.*, **27**, 87 (1967).
[36] M.H. Yu, L.B. Liu, S. Wang. *J. Polym. Sci., Part A: Polym. Chem.*, **46**, 7462 (2008).
[37] J.R. Lakowicz, G. Webber. *Biochemistry*, **12**, 4161 (1973).
[38] X.L. Xi, M.M. Yang, C.Y. Zhou, J. Zhao, P. Yang. *Chin. Sci. Bull.*, **51**, 2322 (2006).
[39] L.M. Chen, J. Liu, J.C. Chen, C.P. Tan, S. Shi, K.C. Zheng, L.N. Ji. *J. Inorg. Biochem.*, **102**, 330 (2008).
[40] S. Satyanarayana, J.C. Dabrowiak, J.B. Chaires. *Biochemistry*, **31**, 9319 (1992).